CONEM 2010
VI Congresso Nacional de Engenharia Mecânica

ABCM COMPROMETIDA COM A PROMOÇÃO DO DESENVOLVIMENTO DA ENGENHARIA E DAS CIÊNCIAS MECÂNICAS
ASSOCIAÇÃO BRASILEIRA DE ENGENHARIA E CIÊNCIAS MECÂNICAS

VI CONGRESSO NACIONAL DE ENGENHARIA MECÂNICA
VI NATIONAL CONGRESS OF MECHANICAL ENGINEERING
18 a 21 de agosto de 2010 – Campina Grande – Paraíba - Brasil
August 18 – 21, 2010 – Campina Grande – Paraíba – Brazil

COMPUTATIONAL MODELING AND EXPERIMENTAL VALIDATION OF SELF-HEATING EFFECTS IN VISCOELASTIC MATERIALS

Jean de Cazenove, jcazenove@mecanica.ufu.br[1]
Antônio Marcos Gonçalves de Lima, amglima@mecanica.ufu.br[1]
Domingos Alves Rade, domingos@ufu.br[1]
Cleudmar Amaral de Araújo, cleudmar@mecanica.ufu.br[1]

[1]Faculdade de Engenharia Mecânica, Universidade Federal de Uberlândia - P.O. Box. 593 - CEP: 38400-902 Uberlândia-MG

Abstract. *Viscoelastic materials have been widely used over the last two decades for passive noise and vibration damping in several kinds of machines, vehicles, industrial equipments and structures. However, only recently the progess in the field of material technology, combined to the apparition of more efficient techniques for numerical modeling and experimental characterization of viscoelastic behaviour of systems equipped with viscoelastic elements permitted to extend the applications of these materials to complex industrial systems. A natural extension of the already obtained advances consists in developing procedures for numerical modeling and experimental characterization of the excitation frequency and temperature effects on the performance of viscoelastic dispositives. In particular, there is great interest in predicting the effects of internal self-heating effects of these materials when applied as passive constrained layer or discrete dispositives, and subjected to diferent kinds of cyclic loads, since heating leads to modifications of the mechanical properties of the material due to the intern processes of relaxation and fluency, affecting the damping capacity of these materials. In this context, the present work presents the development and validation of a finite-element based computational modeling procedure, with the use of the comercial FE code* ANSYS ™ *, to characterize the internal self-heating effect of viscoelastic materials submitted to cyclic excitations. The present work focuses on discrete viscoelastic dispositives such as rotational mounts and translational joints. The treatment of the thermoviscoelasticity problem consists in an iterative procedure in which structural and thermal analyses are sequentially performed, with the actualization of the mechanical properties of the viscoelastic material in function of the temperature.*

Keywords: *damping, passive vibration control, thermoviscoelasticity, finite elements.*

1. INTRODUCTION

Self-heating effects occur when dynamic loads are applied over viscoelastic materials and are caused by the conversion of a part of the strain energy into heat. The resulting temperature field values depend both on operating factors (strain rate and amplitude), structure configuration (contact surfaces for heat exchange) and material parameters (loss factor, thermal conductance, specific heat and thermal conversion ratio). Several analytical and experimental studies have shown that cyclic load cause continous temperature increases and reach critical values ((Merlette, 2005)). As recalled by (Lesieutre and Govindswamy, 1995), the evolution of the temperature field can result in two distinct phenomena, namely: a) the thermal equilibrium, which occurs after a large number of cycles if the influence of the reached temperature field on the mechanical properties is small enough. In this configuration, since the pseudo-equilibrium is reached, the temperature gradually increases at a very small rate until the load is removed b) the "thermal runaway", which happens when the heat generation is large enough to cause chemical reactions which causes material softening and may result into irreversible degradation of the structure.

Only few studies present modeling strategies for the simulation of self-heating effects, since the problem involves the resolution of coupled transient thermal and structural equations. (Gopalakrishna and Laï, 1998) presented an iterative methodology to determine the equilibrium temperature field inside a translational joint. Rittel (1999) defined the heat source as a fraction β of the mechanical power dissipated by the viscoelastic effect, and has shown through the application of cyclic loads over polymeric samples that β values depend on the strain rate and amplitude. Merlette (2005) recalled that usual β values for most viscoelastic polymers are comprised between 0,1 and 1 and identified a set of β values corresponding to a series of tests performed with translational mounts. The curve-fitting procedure was based on the use of a simplified 4-DOF thermomechanical model.

Further sections of this paper present the basic concepts of viscoelastic behaviour in the frequency domain and in-

troduce the analytical expression of the transient heat equation. Subsequently, the experimental results are presented and the influence of the strain amplitude over self-heating is discussed. Finally, the curve-fitting procedure and results are presented.

2. THEORETICAL BACKGROUND

This section is devoted to the description of the dynamic behaviour of viscoelastic materials and obtention of the transient heat equation for the coupled thermomechanical problem. In this particular case, the viscoelastic dissipative effect is taken into account and the expression of the heat generation rate is obtained from the analytical expression of the dissipated power.

2.1 Viscoelastic material modeling approach

The response of viscoelastic materials to imposed loads and displacements is characterized by a delay with respect to the sollicitation. In the case of constant loads imposed over a significant time range, the material response can be adequately represented by a relaxation function, whereas in the case of more complex, time-varying sollicitations, the whole strain history has to be taken into account to establish the stress-strain relationship. For linear viscoelastic materials, the stress state in the material at time t is equal to the sum of all previous contributions. According to Christensen (1982), the application of this assumption to the case of a continuous strain history between $t = 0$ and t leads to the following convolution integral:

$$\sigma_{ij}(t) = \int_0^t G_{ijkl}(t-\tau)\frac{d\varepsilon_{kl}(\tau)}{d\tau}d\,\tau \tag{1}$$

where $\sigma_{ij}(t)$ and $\varepsilon_{kl}(\tau)$ are the stress and strain tensor expressed at time t and τ. $G_{ijkl}(t-\tau)$ is the fourth-order *relaxation tensor* at time $t-\tau$. The variable τ is used to describe the summation of infinitesimal contributions over the entire time range. Eq. (1) can be used to represent the transient behaviour of viscoelastic materials under continuous time-varying sollicitations. However, its use is unnecessary when the material response to a cyclic load reaches the harmonic steady state oscillation condition after an accomodation phase. Christensen shows that, for this particular case, the stress-strain constitutive relationship in the frequency domain can be writtem in terms of a complex, frequency-dependent relaxation tensor through the application of the Fourier transform to Eq. (1):

$$\hat{\sigma}_{ij}(\omega) = G^*_{ijkl}(\omega)\hat{\varepsilon}_{ij}(\omega) \tag{2}$$

where $\hat{\sigma}_{ij}(\omega)$ and $\hat{\varepsilon}_{ij}(\omega)$ are the stress and strain tensors expressed in the frequency domain. According to Nashif *et al.* (1985) the one dimensional-stress-strain relationship can be expressed in terms of the *complex modulus* $E^*(\omega)$ through the following form:

$$\hat{\sigma}(\omega) = E^*(\omega)\hat{\varepsilon}(\omega) = E^{'}(\omega) + iE^{''}(\omega) = E^{'}(\omega)\left[1 + i\eta(\omega)\right] \tag{3}$$

where $E^{'}(\omega)$ and $E^{''}(\omega)$ are the *storage* and *loss* moduli of the viscoelastic material and represent, namely, the elastic and dissipative behaviour of the viscoelastic material. As shown by Eq. (3) is is possible to factor out the storage modulus from the complex modulus expression and express its imaginary part in terms of the loss factor, which corresponds to the ratio of the loss and storage moduli. Recalling that in the case of steady-state harmonic loads $\hat{\varepsilon}(\omega) = \varepsilon_0 e^{i\omega t}$ and through elementary algebric manipulations, one can show that the stress response lags the strain by a phase angle δ whose value is linked to the complex modulus magnitude and phase as follows:

$$E^{'}(\omega) = \frac{\sigma_0}{\varepsilon_0}\cos\delta \tag{4a}$$

$$E^{''}(\omega) = \frac{\sigma_0}{\varepsilon_0}\sin\delta \tag{4b}$$

$$\eta(\omega) = \tan\delta \tag{4c}$$

Fig. (1) illustrates the delay between stress and strain responses for a viscoelastic material submitted to a harmonic load and shows the *histeresis loop* obtained by plotting the stress versus strain. As recalled by Nashif *et al.* (1985), the area inside the hysteretic loop represent the energy dissipated within each vibration cycle.

2.2 Thermoviscoelastic behaviour

According to Rittel (1999), the transient heat equation can be written as follows:

$$q_g + k\nabla^2 T = \rho c_P \dot{T} + (3\lambda + 2\mu)\alpha T_0 \dot{\varepsilon}_{kk} \tag{5}$$

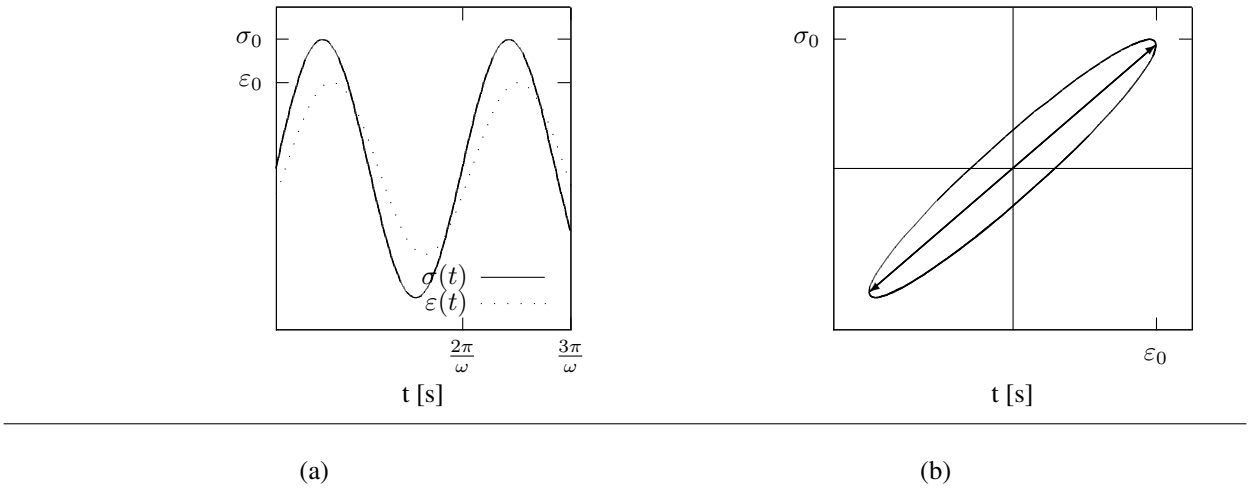

(a) (b)

Figure 1. **Harmonic stress and strain versus time (a) and elliptical histeresis loop (b) for a linear viscoelastic material**

In Eq. (5), k, ρ, c_P and α are namely the heat conductance, density, specific heat and thermal expansion coefficient of the material. T_0 is the reference temperature, λ and μ are the Lamé coefficients and $\dot{\varepsilon}_{kk}$ is trace of the strain rate tensor. $k\nabla^2 T$ represents the heat conduction and is obtained by applying Fourier's law to an infinitesimal volume (Lienhard and Lienhard (2004)), while the rightside terms $\rho c_P \dot{T}$ and $(3\lambda + 2\mu)\alpha T_0 \dot{\varepsilon}_{kk}$ represent namely the heat storage and thermoelastic contribution. The latter terms are obtained by applying the second law of thermodynamics (Gaskell (2003)) and writing the pression field in terms of the stress tensor. The heat generation rate, designed by q_g in Eq. (5), depends on the dissipated mechanical power $\dot{w}_m$:

$$q_g = \beta \dot{w}_m \tag{6}$$

where β represents the ratio of the heat source to the dissipated mechanical work per time unit. According to Rittel (1999) and Rittel (2000), the complementary part of the dissipated power $(1-\beta)\dot{w}_m$ is stored into the viscoelastic material through microstructural changes and the value of β for most viscoelastic polymers depends both on strain amplitudes and strain velocity.

The dissipated mechanical power can be expressed as the scalar product of the stress components vector $\{\sigma(t)\}$ by the strain rate vector $\{\dot{\varepsilon(t)}\}$:

$$\begin{aligned} \dot{w}_m &= \{\sigma(t)\}^T \{\dot{\varepsilon(t)}\} \\ &= \{\varepsilon(t)\}^T \mathcal{H}^*(\omega, \mathcal{T}) \{\dot{\varepsilon(t)}\} \end{aligned} \tag{7}$$

The Poisson ratio is considered to be frequency-independent as a first approximation. Thus, by assuming material isotropy, one can factor out the complex modulus from the elasticity matrix and rewrite Eq. (8) in terms of the complex modulus and normalized elasticity matrix $\overline{\mathcal{H}}$:

$$\dot{w}_m = E^*(\omega, T) \{\varepsilon(t)\}^T \overline{\mathcal{H}} \{\dot{\varepsilon(t)}\} \tag{8}$$

Writing Eq. (8) for the case of cyclic stress-strain states for which $\{\dot{\varepsilon(t)}\} = i\omega\{\varepsilon(t)\}$ leads to a complex expression of $\dot{w}_m$, whose real and imaginary parts are respectively proportionnal to the loss and storage moduli:

$$\dot{w}_m = \underbrace{i\omega \{\varepsilon(t)\}^T \bar{\mathcal{H}} \{\varepsilon(t)\} E^{'}(\omega, T)}_{\dot{w}_{mi}} - \underbrace{\omega \{\varepsilon(t)\}^T \bar{\mathcal{H}} \{\varepsilon(t)\} E^{''}(\omega, T)}_{\dot{w}_{mr}} \tag{9}$$

At this stage $\{\varepsilon(t)\}$ should be written in term of the strain amplitude components vector $\{\varepsilon_0\}$ multiplicated by a sinusoidal factor to describe its variation over time:

$$\{\varepsilon(t)\} = \{\varepsilon_0\} \sin(\omega t + \delta) \tag{10}$$

where δ is the lag between strain and stress. Therefore it is possible to show that the imaginary contribution $\dot{w}_{mi}$ to the viscoelastic dissipation equals to 0 over a vibration cycle:

$$\int_t^{t+2\pi/\omega} \dot{w}_{mi} dt = \int_t^{t+2\pi/\omega} \{\dot{\varepsilon(t)}\}^T \bar{\mathcal{H}} \{\varepsilon(t)\} E^{'}(\omega, T)\, dt \tag{11}$$
$$= \omega \{\varepsilon_0\}^T \bar{\mathcal{H}} \{\varepsilon_0\} E^{'}(\omega, T) \underbrace{\int_t^{t+2\pi/\omega} \sin(\omega t + \delta)\cos(\omega t + \delta)\, dt}_{0}$$

$\dot{w}_{mi}$ represents the purely elastic power stored by the material. On the other hand, $\dot{w}_{mr}$ corresponds to the viscous power and thus represents the nonzero contribution to viscoelastic dissipation:

$$\dot{w}_m = \dot{w}_{mi} \tag{12}$$
$$= -\omega \{\varepsilon_0\}^T \bar{\mathcal{H}} \{\varepsilon_0\} E^{''}(\omega, T) \sin^2(\omega t + \delta)$$

showing that the viscoelastic dissipated power is not constant over a vibration cycle and that its variation depends on the strain amplitude at each time instant. Using this form of Eq. (12) to compute the heat generation rate for the thermomechanical coupled-field analysis would result in a high computational cost since at least 10 time steps by period would be necessary for the time integration of Eq. (12); moreover, significant evolutions of the transient temperature field usually can be observed only on much wider time scales than for mechanical phenomena.

To avoid further useless computational issues it is possible to rewrite Eq. (12) substituting the amplitude factor $\sin^2(\omega t + \delta)$ by the average value of the quadratic sine function:

$$\dot{w}_m = -\frac{1}{2}\omega E^{''}(\omega, T) \{\varepsilon_0\}^T \bar{\mathcal{H}} \{\varepsilon_0\} \tag{13}$$

and obtain the following expression for the heat generation rate:

$$q_g = |\beta \dot{w}_m| = \frac{1}{2}\beta\omega E^{''}(\omega, T) \{\varepsilon_0\}^T \bar{\mathcal{H}} \{\varepsilon_0\} \tag{14}$$

Finally, introducing Eq. 14 in 5:

$$\frac{1}{2}\beta\omega E^{''}(\omega, T) \{\varepsilon_0\}^T \bar{\mathcal{H}} \{\varepsilon_0\} + k\nabla^2 T = \rho c_P \dot{T} + (3\lambda + 2\nu)\alpha T_0 \dot{\varepsilon_{kk}} \tag{15}$$

In the present case, the viscoelastic layers of the damping device are submitted to shear loads only, so that normal strain components can be considered to be null. The transient heat equation can now be rewritten in the following form:

$$\frac{1}{2}\beta\omega E^{''}(\omega, T) \{\varepsilon_0\}^T \bar{\mathcal{H}} \{\varepsilon_0\} + k\nabla^2 T = \rho c_P \dot{T} \tag{16}$$

3. EXPERIMENTAL STUDY

3.1 Dispositive

Fig. 2 shows the complete experimental test dispositive. The test sample consists in a translational damper formed by two *3M VHB 9469 ™* 5 mm thick viscoelastic layers stuck between three steel blocks. The blocks were bolted to a rigid frame that was inserted in the universal test *MTS ™* machine.

As shown by Fig. 2 the temperature inside the viscoelastic layers has been measured by 6 copper-constantan thermocouples. As the 1mm thick viscoelastic foils were stuck together to form the final viscoelastic layers, the thermocouples were inserted at 6 pre-defined positions. The thermocouples were linked to an *Agilent 34970 A* signal analyzer.

3.2 Results

6 tests were performed, each one consisting in applying a vertical displacement $v(t) = v_0 \sin(2\pi f t)$ during 3360 seconds by means of a tensile machine. The thermal aquisition system was set to read and store the temperature values with a two seconds resolution, during the loading phase and after the removal of the imposed displacement in order to capture local temperature evolutions during the unloading phase.

Tab. 1 shows the frequency and amplitude values associated to each test.

Fig. 3 shows the temperature measured by the thermocouple T2 for each test. T2 was localized at the mid-point of a transverse (i.e., paralel to the viscoelastic layer main section) plane that was 1mm distant from the central steel block. It can be seen that the imposed displacement amplitude has a strong influence over the temperature values reached due to self-heating effects; it can also be noted that all test curves permit to identify a progressive stabilization of the temperature during the loading phase and a strong and immediate decrease of the temperature values after the removal of the loads.

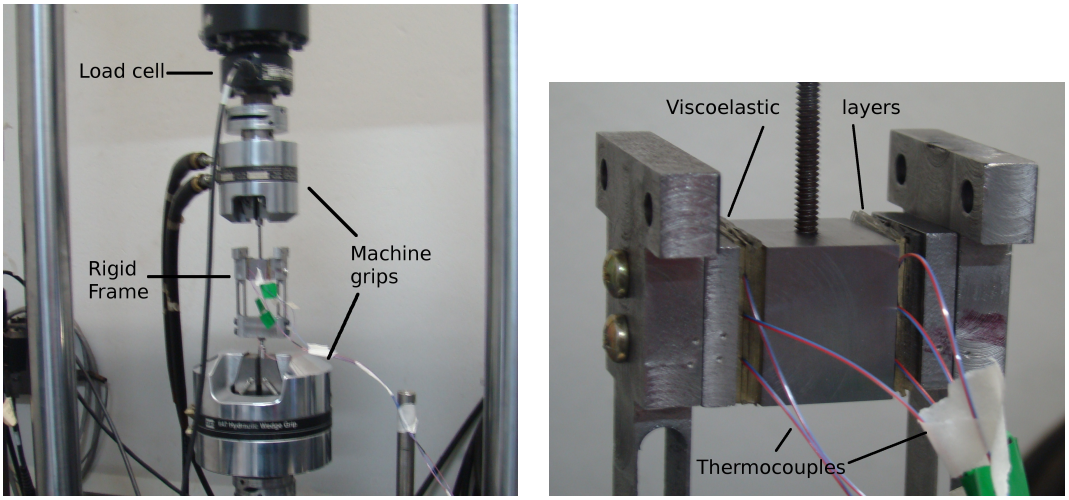

(a) (b)

Figure 2. **Detailed view of the experimental apparatus (a) and of the test sample (b)**

Table 1. Description of the test parameters

Test	a	b	c	d	e	f
f [Hz]	10			15		
v_0 [mm]	0,5	1	1,5	0,5	1	1,5

4. NUMERICAL SIMULATION

4.1 Incorporation of the viscoelastic behaviour into FE models

Considering a viscoelastic element, the integration of the movement equation in the frequency domain leads to the following equation:

$$\left([K^*(\omega,T)]_{(e)} - \omega^2[M]_{(e)}\right)\{u(\omega)\}_{(e)} = \{f(\omega)\}_{(e)} \tag{17}$$

were $[K^*(\omega,T)]_{(e)}$ is the complex, temperature and frequency-dependent stiffness matrix of the element since the behaviour of the viscoelastic material is represented by the complex modulus. Elementar matrix assembly permit the obtention of the global, finite-element discretized system:

$$\left([K_e] + [K_v^*(\omega,T)] - \omega^2[M]\right)\{u(\omega)\} = \{f(\omega)\} \tag{18}$$

where $[K_e]$ and $[K_v^*(\omega,T)]$ correspond, namely, to the elastic and real stiffness matrix, associated to purely elastic DOFs, and to the complex stiffness matrix, associated to viscoelastic DOFs. By assuming a temperature and frequency-independent Poisson ration and for isotropic materials (de Lima and Rade (2005)) the complex modulus can be factored out the complex stiffness, introducing the normalized, temperature and frequency independent stiffness matrice $[\bar{K_v}]$:

$$[K_v^*(\omega,T)] = E^*(\omega,T)[\bar{K_v}] = E^{'}(\omega,T)\left(1 + i\eta(\omega,T)\right)[\bar{K_v}] \tag{19}$$

where the imaginary part of $[K_v^*(\omega,T)]$ represents the proportional damping matrix of the system. The implementation of material dissipative behaviour in most commercial FE codes is realized through an equivalent viscous damping matrix, formulated as follows:

$$[C_{eq}(\omega,T)] = \frac{E^{'}(\omega,T)\eta(\omega,T)}{\omega}[\bar{K_v}] \tag{20}$$

Thus we obtain the global equation of the structural harmonic finite-element subproblem:

$$\left([K_e] + E^{'}(\omega,T)[\bar{K_v}] + i\omega[C_{eq}] - \omega^2[M]\right)\{u(\omega)\} = \{f(\omega)\} \tag{21}$$

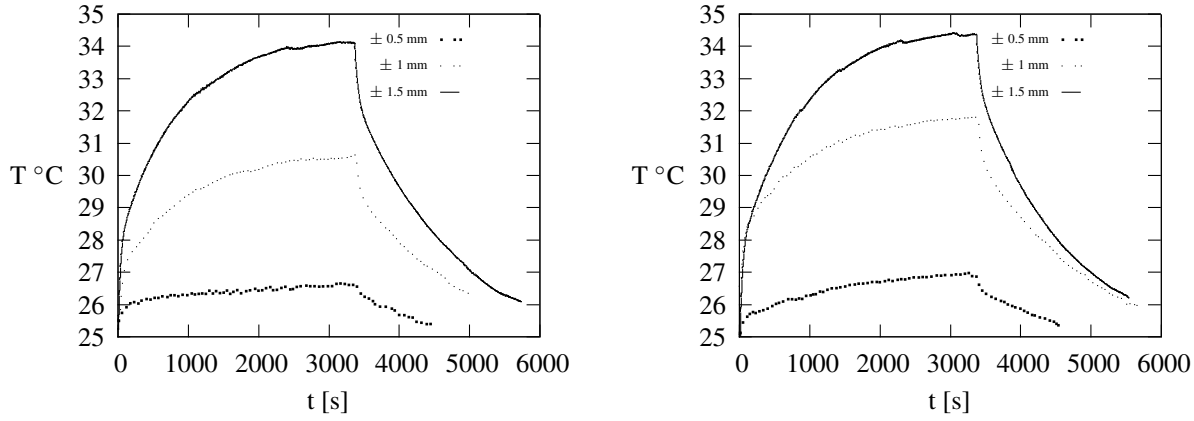

Figure 3. Temperature measured inside the viscoelastic layer for $f = 10$ Hz (a) and $f = 15$ Hz (b)

4.2 Formulation of the heat font in the FE context and sequential iterative solution

This subsection introduces the detailed procedure for the resolution of the thermoviscoelastic coupled problem in the finite element context. Since direct coupling between thermal and structural fields would result in prohibitive computational costs, the problem was solved using a weak coupling procedure in which harmonic structural and transient thermal analyses were performed alternatively. The complete, sequentially-coupled problem is described by the following matricial system:

$$\begin{bmatrix} [0] & [0] \\ [0] & [A] \end{bmatrix} \begin{Bmatrix} \{\dot{u}(\omega_0)\} \\ \{\dot{T}\} \end{Bmatrix} + \begin{bmatrix} [Z^*(\omega_0, T)] & [0] \\ [0] & [W] \end{bmatrix} \begin{Bmatrix} \{u(\omega_0)\} \\ \{T\} \end{Bmatrix} = \begin{Bmatrix} \{f(\omega_0)\} \\ \{q\} + \{q_d\} \end{Bmatrix} \tag{22}$$

in which $[A]$ and $[W]$ are namely the thermal damping and stiffness matrix, whose formulation is based on the thermal elements shape functions and on the specific heat and thermal conductivity, which are considered to be temperature-independent in this application. $Z^*(\omega_0, T) = [K_e] + E^{'}(\omega_0, T)[\bar{K}_v] + i\omega_0[C_{eq}] - \omega^2[M]$ is the complex dynamic stiffness matrix that represent the mechanical behaviour of the structure for a constant frequency ω_0 at temperature T. $\{q\}$ is the vector of thermal loads obtained from boundary conditions and $\{q_d\}$ represents the nodal heat generation vector, obtained from the strain energy whose calculation is based on the structural response. In the *ANSYS* TMFE code the heat generation rate has to be defined for each viscoelastic element. The following expression for element heat generation can be obtained by integrating the heat generation rate defined in Eq. (14) over the element volume:

$$q_{(e)} = \frac{1}{2} \frac{\beta \omega_0 \eta(\omega_0, T)}{V_{(e)}} \{u\}^T_{(e)} [K_v(\omega_0, T]_{(e)} \{u\}_{(e)} \tag{23}$$

where $[K_v(\omega_0, T]_{(e)}$ is the real part of the element complex stiffness matrix and $V_{(e)}$ is the volume of the element. Eq. (23) corresponds to an approximate definition of the heat generation rate since its value is considered to be uniform within the element volume. However the comparison of the model to experimental results tend to prove that the relative error due to the heat source calculation is neglectible for a sufficiently refined mesh.

Fig. 4 represents the iterative solution flowchart for the iterative solution. The resolution of the problem has been implemented using the *APDL* (*Ansys Parametric Design Language*) code, which is a built-in programmation language for the *ANSYS* TM software.

4.3 Curve-fitting procedure

In the previous subsection the finite element formulation for the thermoviscoelastic sequentially coupled analysis has been presented. Direct comparison of the model to experimental results is not possible since there is no data available for the values of two parameters, namely the thermal conversion ratio β and the film coefficient for natural convection heat transfer h. In order to identify the values of these parameters, a curve-fitting procedure has been developed, based on the thermomechanical simulation tool. An optimization routine was used to minimize an objective function defined as the sum of the squares of the offsets of the numerical solution to the experimental points.

The differential evolution method, based on genetic algorithms, was chosen to adjust the model, with β and h as the optimization variables. Fig. 5 represents the finite element model of the test sample, using the following *ANSYS* TMfinite elements:

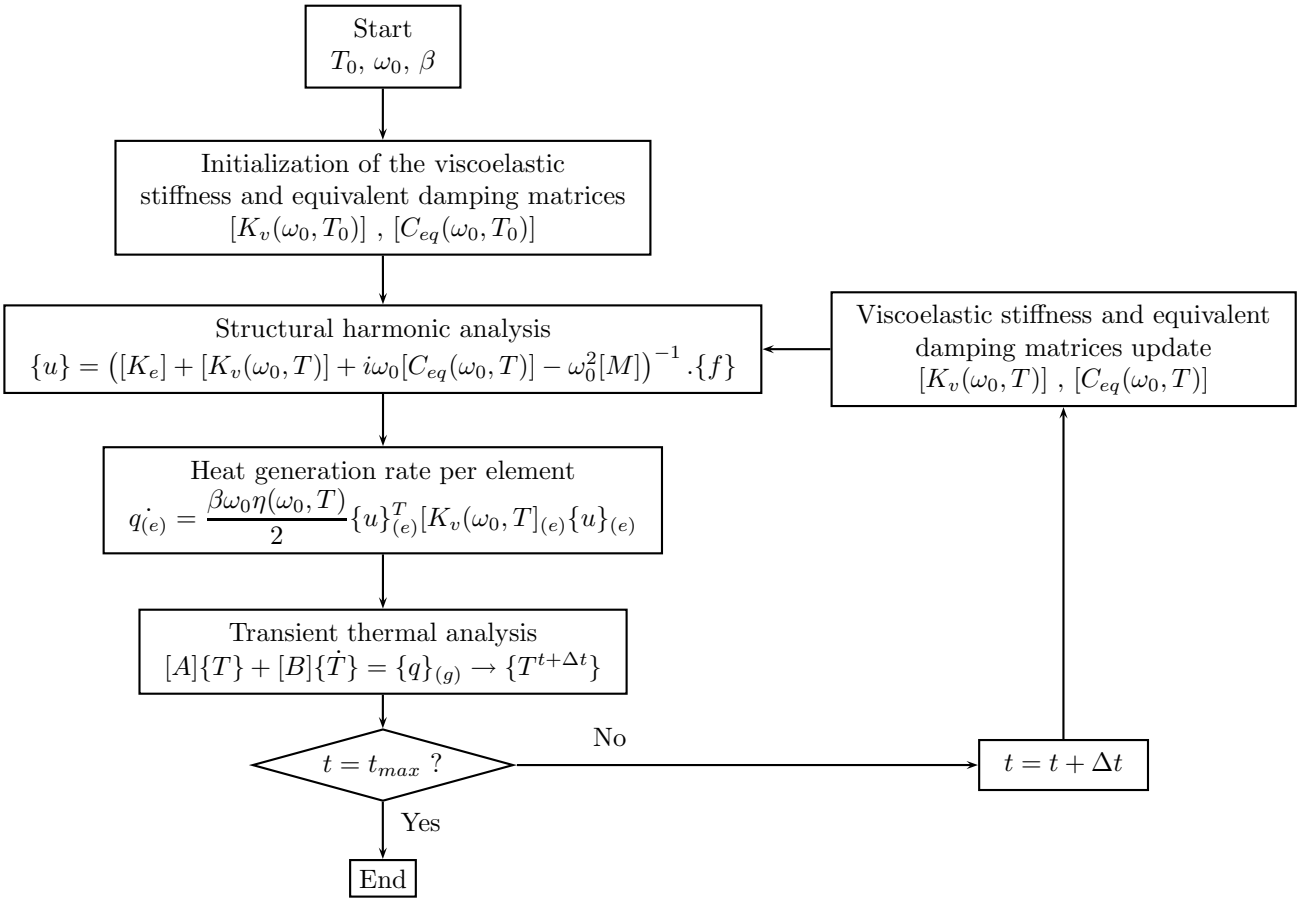

Figure 4. **Flowchart for sequentially coupled thermomechanical self-heating analysis**

- SOLID45, used for the structural subproblem, is a 8-node volume element having 3 DOFs per node, namely the x, y and z displacements;
- SOLID70, used for the thermal subproblem, is a 8-node volume element having 1 DOF (the temperature) per node.

From Fig. 5 it can be seen that only half of the domain corresponding to the test sample has been modeled due to a symmetry with respect to the mid-plane. This required the application of the following specific boundary conditions on the symmetry plane (an null heat flux and prohibited normal displacements).

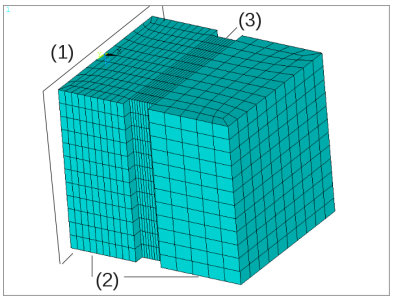

(1) Symmetry plane
(2) 1020 Steel
(3) *3M VHB 9469* ™

Figure 5. **Finite element model of the test sample**

Tab. (2) contains the thermal properties values for the 1020 steel and *VHB 9469* viscoelastic material.

A table containing the complex modulus values for the simulation frequencies (10 and 15 Hz) and for the temperature range $[25^\circ\ \mathrm{C} : 50^\circ\ \mathrm{C}]$ was defined by polynomial interpolation from the *VHB 9469* nomograph presented by Fig. (6).

Table 2. **Thermal properties for the 1020 steel and the *VHB 9469* viscoelastic material**

Material	k [W.m^{-1}.K^{-1}]	ρ [kg.m^{-3}]	c_P [J.kg^{-1}.K^{-1}]
1020 Steel	35	7850	476
VHB 9469	0.16$^{(1)}$	1000$^{(1)}$	2000$^{(2)}$

$^{(1)}$ from the *3M* technical bulletin, 2003
$^{(2)}$ from Merlette, 2005

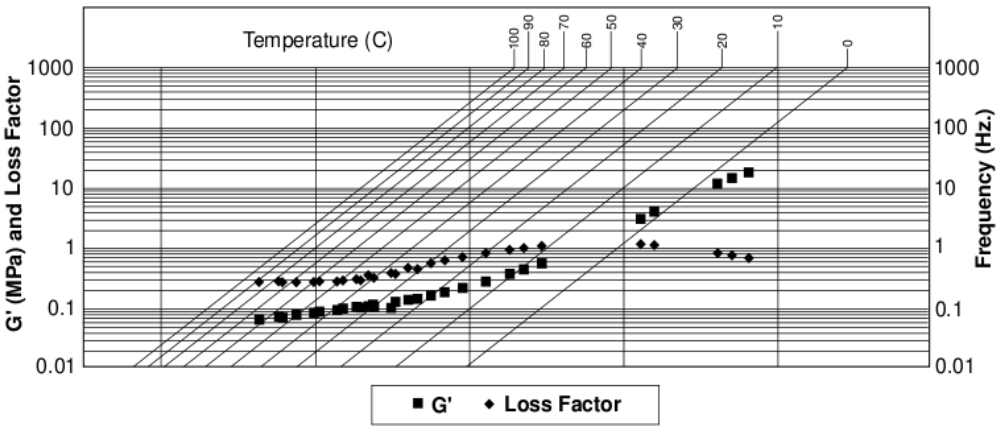

Figure 6. ***3M VHB 9469* ™ nomograph. Source: *3M* ™ Technical Bulletin (2003)**

4.4 Results

This subsection presents the results of the curve-fitting procedure applied to the finite element model. The results of test *b* , obtained with $v_0 = 1$ mm and $f = 10$ Hz, has been used to identify the h and β values. After 50 evaluations of the objective function, the optimal values of $h_{opt} = 13.016$ W.m^{-2}.K^{-1} and $\beta_{opt} = 0,1755$ were found. Figure (7) presents the experimental temperature measured by thermocouples T2 for test *b* and the numerical solution obtained with the optimal values h_{opt} and β_{opt}.

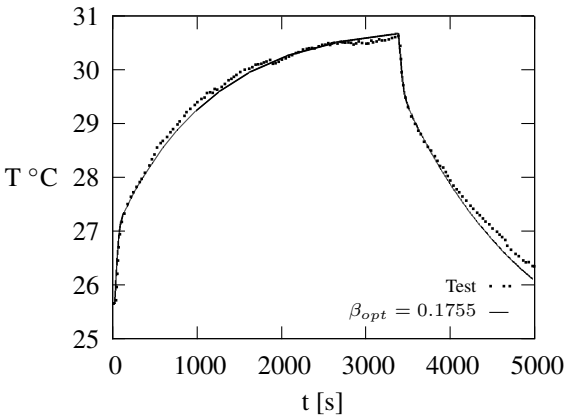

Figure 7. **Curve fitting result for test *b***

For the tests *a*, *c*, *d*, *e* and *b* the values of β were fitted to test results considering $h = h_{opt}$. For each test, the optimal value of β was identified through an iterative reduction of the search interval, using the golden section algorithm. As shown by Fig. (8), the search interval has been determined previously by manual adjustment of the model in order to reduce the number of iterations for the identification of β.

Table (3) shows the β_{opt} values for each test. It can be seen that the higher the strain amplitude, the lower the value of β. A similar trend had been observed by (Merlette, 2005), and can be explained by the fact that the complementary part of the dissipated power is stored in the material through microstructural changes. Consequently, a higher the strain amplitude would result into more important modifications in the material microstructure, accounting for a lower fraction

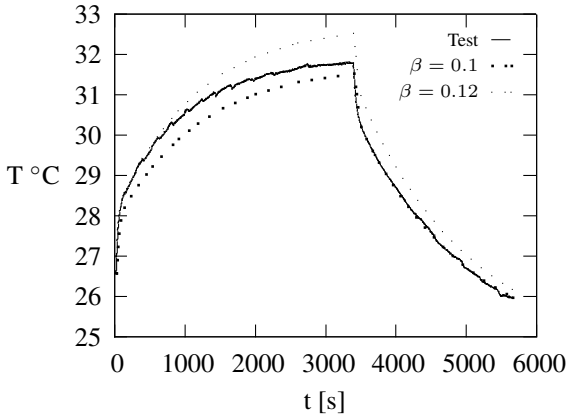

Figure 8. **Illustration of the search interval reduction for test *e*, with β_{min} =0,1 and β_{max} =0,12**

of the dissipated energy converted into heat.

Table 3. β_{opt} values

f [Hz]	10			15		
v_0 [mm]	0.5	1	1.5	0.5	1	1.5
β_{opt}	0.2055	0.1755	0.15	0.1324	0.1079	0.0771
F_{obj}	10.8141	15.5463	65.2724	7.5945	35.1145	137.6865

Figures (9) and (10) present the results of the curve-fitting procedures for test *a*, *d*, *c* and *f*. It can be seen from Fig. (9) that, for tests *a* and *d*, the noise on the experimental curve, which is probably due to the acquisition equipement, is more visible since the self-heating effects are less important.

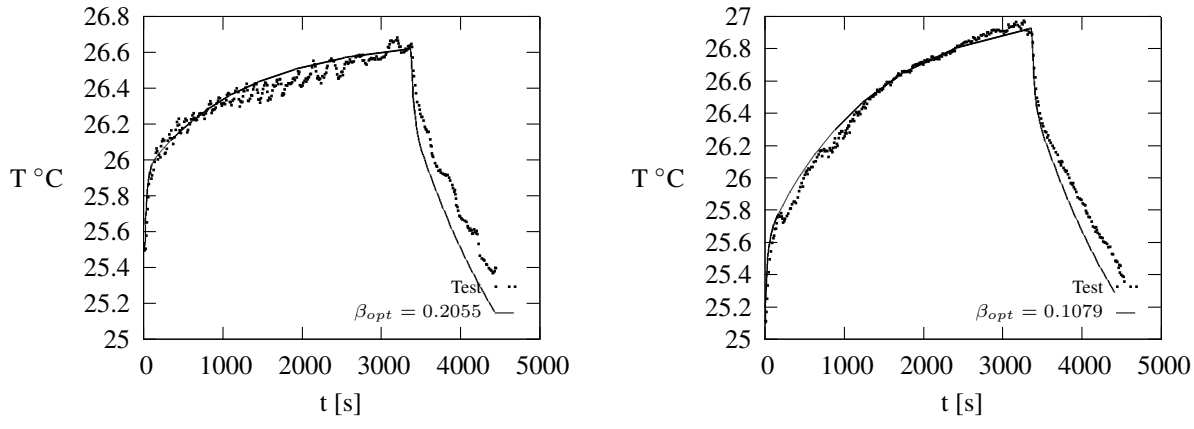

(a) (b)

Figure 9. **Curve-fitting results for tests *a* (a) and *d* (b)**

5. CONCLUSION

In this paper, a procedure for coupled self-heating effects finite-element modeling has been proposed and succesfully compared to experiment results. However it should be noticed that the values of β obtained through the curve-fitting procedure are lower than the values observed by Merlette, for a similar material. This difference can be explained by the fact that the test sample was formed by laminates, turning inhomogeneous the viscoelastic layers, and that losses of energy may have occured at the interfaces between the laminates. In further works, the same kind of experiments should be performed with homogeneous blocks of viscoelastic materials, which may turn more difficult the insertion of the

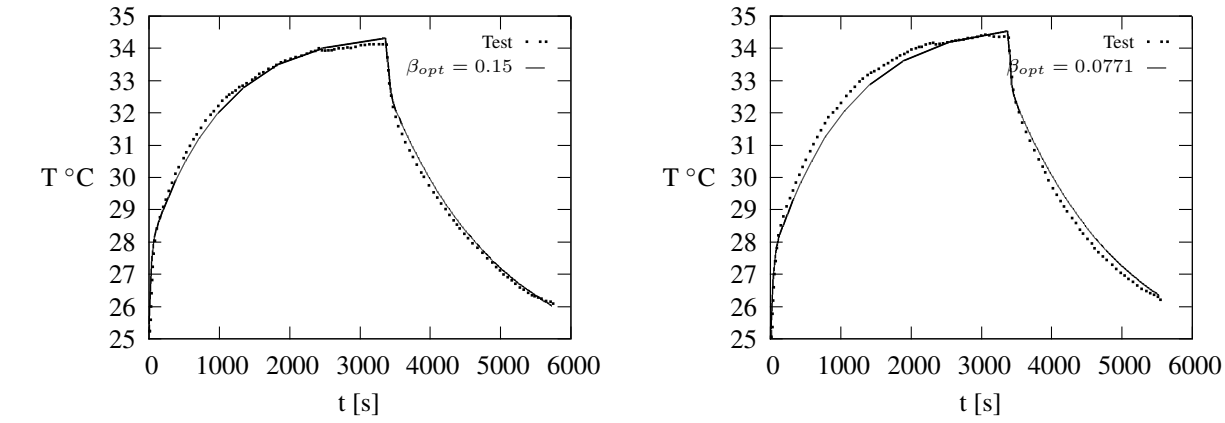

Figure 10. **Curve-fitting results for tests *c* (a) and *f* (b)**

thermocouples in the viscoelastic material but, on the other hand, would result in a more reliable experimental-numerical comparison.

6. ACKNOWLEDGEMENTS

The authors gratefully acknowledge the following organizations for the continued support to their research work:

- CNPq - Brazilian Research Council, especially for Prof. Rade's research grant (processo 310524/2006-7), Prof. Lima's project 480785/2008-2 and Mr. de Cazenove M.Sc. Master Scholarship.
- Minas Gerais State Research Agency FAPEMIG.
- CAPES Foundation, of the Brazilian Ministry of Education.

7. REFERENCES

Christensen, R.M., 1982. *Theory of Viscoelasticity - An Introduction*. Academic Press, New York, USA.

de Lima, A.M.G. and Rade, D.A., 2005. "Modeling of structures supported on viscoelastic mounts using frf substruturing,". In *Proceedings of the Twelfth International Congress on Sound and Vibration*. Lisbon, Portugal.

Gaskell, D.R., 2003. *Introduction to the Thermodynamics of Materials - Fourth Edition*. Taylor & Francis, Cambridge, USA.

Gopalakrishna, H.S. and Laï, M.L., 1998. "Finite element heat transfer analysis of viscoelastic damper for wind applications,". *Journal of Wind Engineering and Industrial Aerodynamics*, Vol. 77 & 78, pp. 283–295.

Lesieutre, G.A. and Govindswamy, K., 1995. "Finite element modeling of frequency-dependent dynamic behavior of viscoelastic materials in simple shear,". *International Journal of Solids and Structures*, Vol. 33, pp. 419–432.

Lienhard, J.H.I. and Lienhard, J.H.V., 2004. *A Heat Transfer Textbook - Third edition*. Phlogiston Press, Cambridge, USA.

Merlette, N., 2005. *Amortissement des Caisses Automobiles par des Films Minces Viscoélastiques pour l'Amélioration du Confort Vibratoire*. Ph.D. thesis, École Centrale de Lyon, Lyon, France.

Nashif, A.D., Jones, D.I.G. and Henderson, J.P., 1985. *Vibration Damping*. John Wiley and Sons, New York, USA.

Rittel, D., 1999. "On the conversion of plastic work to heat during high strain rate deformation of glassy polymers,". *Journal of Mechanics of Materials*, Vol. 31, pp. 131–139.

Rittel, D., 2000. "An investigation of the heat generated during cyclic loading of two glassy polymers. part i: Experimental". *Journal of Mechanics of Materials*, Vol. 32, pp. 131–147.

8. RESPONSIBILITY NOTICE

The authors are the only responsible for the printed material included in this paper.